A new approach for the design of hypersonic scramjet inlets

N. Om Prakash Raj and K. Venkatasubbaiah

Citation: Physics of Fluids (1994-present) **24**, 086103 (2012); doi: 10.1063/1.4748130
View online: http://dx.doi.org/10.1063/1.4748130
View Table of Contents: http://scitation.aip.org/content/aip/journal/pof2/24/8?ver=pdfcov
Published by the AIP Publishing

A new approach for the design of hypersonic scramjet inlets

N. Om Prakash Raj and K. Venkatasubbaiah[a)]
Department of Mechanical Engineering, Indian Institute of Technology Hyderabad, Hyderabad, Andhra Pradesh 502205, India

(Received 24 April 2012; accepted 1 August 2012; published online 30 August 2012)

A new methodology has been developed for the design of hypersonic scramjet inlets using gas dynamic relations. The approach aims to find the optimal inlet geometry which has maximum total pressure recovery at a prescribed design free stream Mach number. The design criteria for inlet is chosen as *shock-on-lip* condition which ensures maximum capture area and minimum intake length. Designed inlet geometries are simulated using computational fluid dynamics analysis. The effects of 1D, 2D inviscid and viscous effects on performance of scramjet inlet are reported here. A correction factor in inviscid design is reported for viscous effects to obtain *shock-on-lip* condition. A parametric study is carried out for the effect of Mach number at the beginning of isolator for the design of scramjet inlets. Present results show that 2D and viscous effects are significant on performance of scramjet inlet. Present simulation results are matching very well with the experimental results available from the literature. © *2012 American Institute of Physics*. [http://dx.doi.org/10.1063/1.4748130]

I. INTRODUCTION

In the era of hypersonic air breathing propulsion systems, scramjets (supersonic combustion ramjets) play a crucial role in high-speed flight travel. A space vehicle employing scramjet propulsion improves the payload capabilities of the vehicle and thereby increasing the space transportation system efficiency. Scramjet engine consists of no moving parts and the compression process has to be done by shock waves instead of compressor in gas turbine engines. The performance of scramjet propulsion is mainly dependent on the compression process. The inlet of scramjet engine must be designed to improve the compression process and also deliver supersonic air to the combustion chamber. It is required to obtain an optimal design of inlet which has maximum total pressure recovery (TPR) and achieves an adequate compression. Present investigation has been focused to obtain best possible intake geometry for scramjet engines.

Scramjet propulsion system design has been interested of study since past few years and scramjets are preferred when compared to rocket propulsion system because of its light weight, high specific impulse, and greater potential for maneuverability.[1] There are three types of scramjet inlets; (i) external compression inlet, (ii) internal compression inlet, and (iii) mixed compression inlet. Among which, mixed compression inlet has the advantage of having low drag, shorter intake length, and high pressure ratio potential.[2] Mixed compression inlet can be designed by the following two approaches: one aiming at maximizing total pressure recovery and another aims of design at prescribed Mach number at the beginning of isolator. By employing these two approaches independently, supersonic inlet was designed and the effects of on-design and off-design conditions on performance of inlet at different flight Mach numbers were reported.[3]

One of the first attempts in developing an optimal design for supersonic inlet which reduces to subsonic flow was done by Oswatitsch.[4] By using gas dynamic relations and Lagrange multipliers

[a)]E-mail: kvenkat@iith.ac.in.

and with an objective of maximum total pressure recovery, a set of oblique shock angles and one terminating normal shock angle were obtained. It has been observed that in order to improve the compression efficiency, shocks have to be of equal strength (Oswatitsch criterion). Extension of this analogy for scramjet inlet was done by Smart,[5] where the inlet was optimized based on maximum total pressure recovery and Oswatitsch criterion is also observed. It is also found that total pressure recovery increases with an increase in number of shocks.

In another approach, bilevel integrated system synthesis method was used for optimization of scramjet inlet and flow phenomena in three subsystems of scramjet: inlet, combustor, and nozzle were studied using computational fluid dynamics (CFD).[6] Optimization was done using one-dimensional gas dynamic relations. Avoiding the separation region and improvement of scramjet performance were reported using CFD analysis. Another aspect that has to be considered in design of inlet is to establish supersonic flow through the inlet without causing inlet to unstart. These issues are reported[7] and theoretical starting limit known as Kantrowitz limit puts a restriction on area. Kantrowitz limit is defined as ratio of area at the cowl lip to the beginning of isolator. By experiments it is observed that scramjet inlet unstarts if Kantrowitz limit is not satisfied.[8] Inlet unstart is also caused by the presence of separation regions which chokes the scramjet inlet.[9] Mach number at beginning of isolator is also an important parameter for design of inlet because which has significant effect on formation of separation region. The formation of separation regions was observed experimentally[10] if the Mach number at the beginning of isolator is less than 50% of the free stream Mach number. In cases when separation is unavoidable, various methods, such as bleeding or blowing, have been used to control or reduce its influence on the inlet.[11]

Research has also been done in the design of 3D hypersonic inlets.[12] In this study, inviscid stream tracing technique was used for design of inlet with rectangular to elliptical shape transition and is also tested experimentally.[13] Experimental tests were conducted for mixed compression inlet to study the viscous effects on inlet flow field parameters and found that passive bleeding reduces the separation regions.[14] Flow field of external compression inlet was experimentally tested at Mach 10 for a range of cowl positions.[15] It is found that cowl position is one of the important parameter for operation of scramjet inlet. Design requirements of isolator being the system which connects inlet and combustion chamber were reported in the literature.[16] Various experimental and computational investigations were performed to know the effect of isolator lengths on performance of scramjet inlet by Reinartz and Hermann.[17] CFD has evolved up to an extent where complex phenomenon of hypersonic propulsions can be modeled and these CFD simulations have become important means to study the physics of scramjet engines.[18–23] Various numerical techniques have been used to analyze the scramjet propulsion such as large eddy simulation to model the jet injection in scramjet combustion chamber.[24]

However, research has been done by either optimizing total pressure recovery or prescribing Mach number at the beginning of isolator. The objective of present investigation is to intuitively combine the above two methodologies and to obtain an optimal geometry which has maximum total pressure recovery at a prescribed free stream Mach number. A new methodology using gas dynamic relations has been developed to obtain optimal geometry of scramjet inlet at different Mach numbers. *Shock-on-lip* condition which ensures maximum capture area and minimum intake length is one of the important parameters and the geometry is made to satisfy this condition. The performance parameters of inlets have been analyzed using CFD and their corresponding deviations in 1D, 2D inviscid and 2D viscous cases are reported here.

II. DESIGN METHODOLOGY

The present investigation is to design a mixed compression scramjet inlet due to its fore mentioned advantages when compared with external and internal compression inlets. In mixed compression, inlet compression process takes place in two stages (i) external compression and (ii) internal compression. Inlet consist of three parts, namely, forebody, cowl and innerbody as shown in Figure 1. External compression takes place by means of oblique shocks originating from a series of external compression ramps along the forebody and internal compression starts from cowl lip. Innerbody starts at the end of forebody and cowl starts from the cowl tip. Both innerbody and cowl

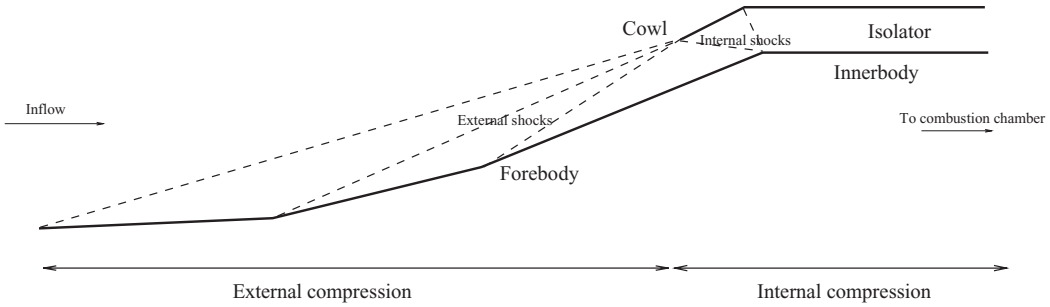

FIG. 1. Schematic of scramjet inlet.

extends to the inlet of combustion chamber. Isolator is the horizontal section between cowl and innerbody. Initially, fluid at a free stream Mach number M_1 passes through series of external shocks and gets decelerated in the process. Then the fluid passes between the cowl and innerbody through a series of internal shocks and in this process flow is further decelerated and then enters into the isolator, through which the compressed flow is delivered into the combustion chamber at supersonic velocities.

The number of external and internal shocks has to be fixed for the design of inlet. The performance of scramjet inlet improves with increase in number of shocks due to increase of total pressure recovery. However, isentropic condition puts a limit on number of shocks.[3] Moreover, increase in number of shocks implies to decrease in ramp angles and thereby increasing the length of the inlet which adds to overall weight of the scramjet.

A. Turning (θ) and shock (β) angles

The number of external/internal shocks determines the number of turning/ramp angles required. By Oswatitsch criterion, in order to increase the efficiency of inlet, pressure jump across a single shock is equally distributed by using multiple shocks with equal strength. The turning and shock angles are obtained iteratively using gas dynamic relations so as to maximize inlet efficiency. Scramjet inlet operates at a free stream Mach number M_1 and Mach number after the internal compression, i.e., at the beginning of isolator is specified as one half of the free stream Mach number in order to avoid flow separation.[10] The Mach number after external compression M_e has been specified as the limiting Mach number after which normal shock is unavoidable, i.e., flow turns sonic.

In this design procedure, external compression and internal compression are divided into two subsystems and flow turning angles are obtained independently. Except that the static pressure ratio after external compression is carried to the internal compression in order to couple two subsystems. At low turning angles, weaker shocks are formed which indicate static pressure ratio is low and total pressure ratio is maximum across the shock. So the initial guess values are chosen as static pressure ratio SPR $= 0.01$ and total pressure ratio TPR $= 1.0$ and the corresponding shock angle, turning angle, Mach number, total pressure ratio across the shock are obtained at a free stream Mach number using the following gas dynamic relations:

$$\beta = \sin^{-1}\left[\sqrt{\frac{\left((\mathrm{SPR}-1)\left(\frac{\gamma+1}{2\gamma}\right)\right)+1}{M_1^2}}\right], \tag{1}$$

$$\theta = \tan^{-1}\left[2\cot\beta\left(\frac{M_1^2\sin^2(\beta)-1}{M_1^2\left(\gamma+\cos 2\beta+2\right)}\right)\right], \tag{2}$$

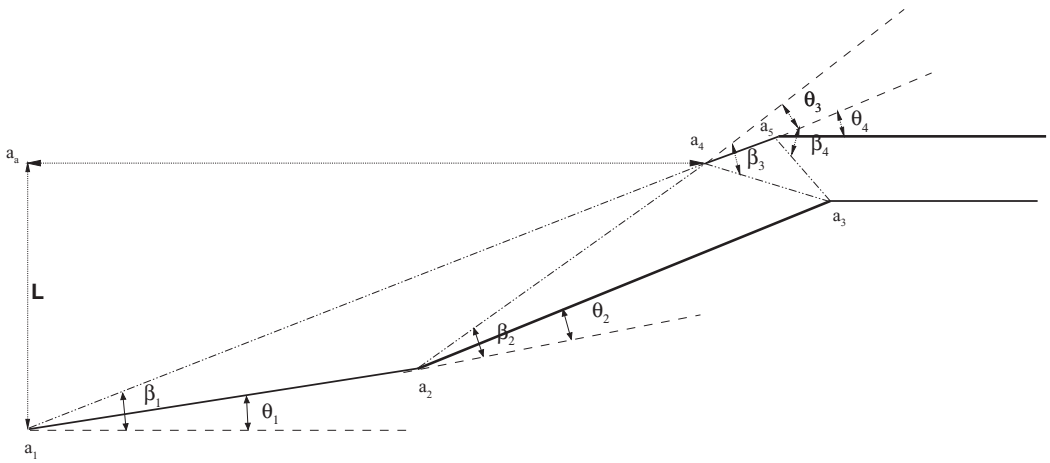

FIG. 2. Geometrical parameters of scramjet inlet.

$$M_2 = \frac{\sqrt{\frac{\left(M_1^2 \sin^2(\beta) + \frac{2}{\gamma-1}\right)}{\left(\frac{2\gamma}{\gamma-1} M_1^2 \sin^2(\beta) - 1\right)}}}{\sin(\beta - \theta)}, \tag{3}$$

$$\text{TPR} = \left[\left(1 + \frac{\gamma-1}{2} M_2^2\right)^{\frac{\gamma}{\gamma-1}} \left(1 + \frac{2\gamma}{\gamma+1}\left(M_1^2 \sin^2(\beta) - 1\right)\right) \left(1 + \frac{\gamma-1}{2} M_1^2\right)^{\frac{-\gamma}{\gamma+1}}\right]. \tag{4}$$

Static pressure ratio of previous shock is fixed for the next shock, and properties behind the shock are obtained using the above gas dynamic relations. The same procedure is repeated for all the external shocks. The Mach number behind the last external shock is compared with the specified Mach number after external compression M_e. If both Mach numbers are equal, then the external turning and shock angles are obtained, otherwise the above procedure is repeated by little increase in static pressure ratio.

Similar procedure has been followed to obtain internal flow turning angles, except that the static pressure ratio obtained in the above procedure is considered as initial guess and properties behind the internal shocks are obtained using the above gas dynamic relations. The iteration process is repeated until the Mach number after internal compression equals to Mach number at the beginning of isolator $M_{is} = 0.5M_1$ which is specified as design criteria to avoid separation. The total pressure ratio/static pressure ratio along the inlet is obtained by multiplying the total pressure ratio/static pressure across all shocks. Finally, optimum turning angles and shock angles are obtained for the prescribed flight Mach number.

B. Inlet geometry

Inlet geometry has been obtained using the set of turning angles and their corresponding oblique shock angles. From Figure 2, a_1a_2 and a_2a_3 are the external ramp angles and a_4a_5 is the internal ramp angle. Turning angles for a_1a_2, a_2a_3, and a_4a_5 are given by $\theta_1, \theta_2, \theta_3$ and shock angles β_1, β_2, β_3, respectively, which are obtained using gas dynamic relations as discussed in Sec. II A. Length L is the reference length depending on design requirements. All the external/internal oblique shocks are made to meet at a single point so as to obtain maximum capture area and to minimize the spillage losses. This condition is called as *shock-on-lip* condition and is necessary to avoid unfavorable flow patterns between shocks. The point a_4 is the cowl lip where the external shocks converges. In order to reduce the inlet length, a_4 chosen as the point where the first external oblique shock meets the horizontal line drawn from a_a. Similarly, a_3 is the point where internal shocks converges. The corresponding ramp lengths and inlet geometry is obtained using trigonometric relations.

III. NUMERICAL METHOD

Two-dimensional Navier-Stokes equations are solved using commercial CFD software FLUENT. Kinetic energy (k)-turbulent dissipation (ϵ) model with renormalization group is implemented. Air is considered as an ideal gas with variable properties. Sutherland law is used to calculate the viscosity and piecewise polynomial is used to calculate temperature dependent specific heat. The boundary conditions at the inflow are specified as free stream operating conditions and the flow variables at the outflow are extrapolated from the interior. No-slip boundary conditions are imposed at the solid walls for velocity field. Constant temperature is used at the solid walls for temperature field. A fine grid is used in the isolator section to capture the shock-shock and shock/boundary layer interactions. Wall $y^+ < 5$ is realized to resolve the gradients near the wall. Numerical simulations are obtained with three different grid sizes: coarse mesh 75 969 cells, medium mesh 184 659 cells, and fine mesh 305 100 cells. Results show grid independency and hence all simulations reported herein with medium mesh. Numerical accuracy of present results has been validated with experimental results reported in literature.[15]

IV. RESULTS AND DISCUSSION

Design of scramjet inlet and flow field characteristics are studied numerically. A new approach has been developed for the design of scramjet inlet and the inlet is tested with CFD analysis. The design Mach number of the scramjet inlet is considered as cruising flight Mach number. The effects of 1D, 2D inviscid and viscous effects on performance of scramjet inlet are reported here.

A. Inlet geometry and 1D inviscid effects

Total pressure recovery coefficient is one of the important performance parameters of scramjet inlet and is defined as the ratio of total pressure at the beginning of isolator to the free stream total pressure (TPR_{is}) or total pressure at the exit of isolator to the free stream total pressure (TPR_{exit}).

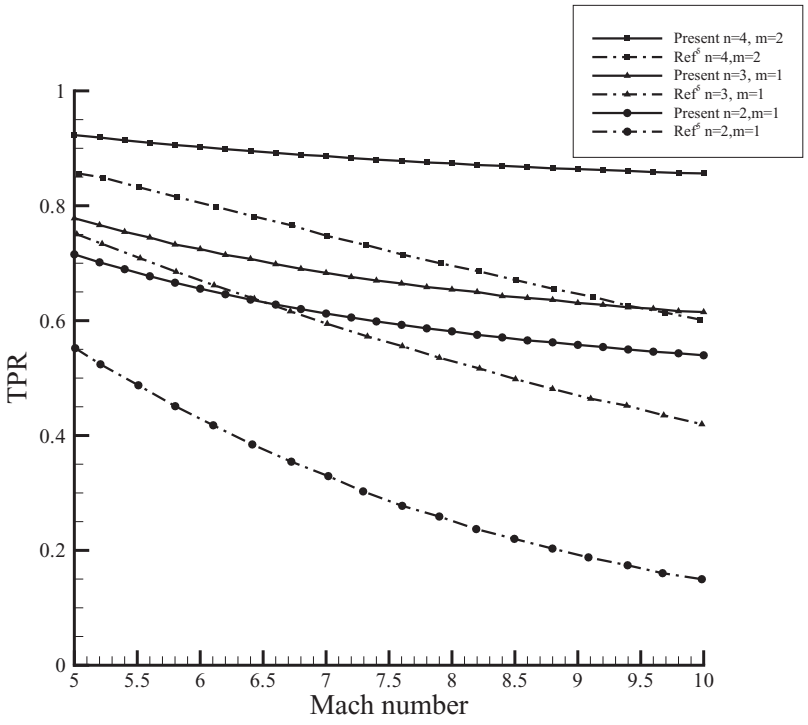

FIG. 3. Variation of total pressure recovery with Mach number.

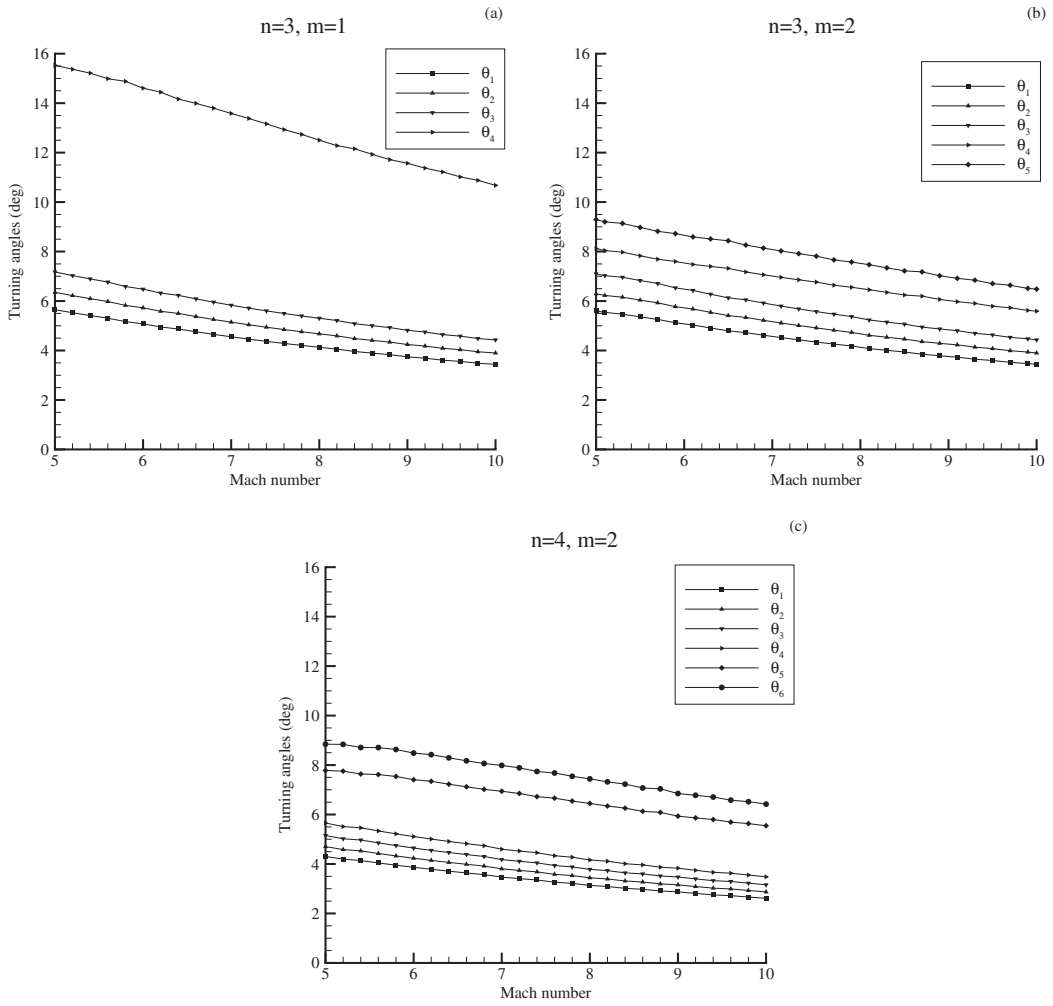

FIG. 4. Turning angles at various Mach numbers for different combinations of external and internal shocks.

Total pressure recovery coefficient for 1D inviscid case is obtained using gas dynamic relations as discussed in Sec. II for different combinations of external shocks (n) and internal shocks (m).

Variation of TPR with different free stream Mach numbers is shown in Figure 3 for different combinations of external and internal shocks. TPR increases with an increase of external or internal shocks due to decrease of shock strength. Present results have been compared with results reported with an approach of optimum total pressure recovery by Smart.[5] From Figure 3, it can be noticed that the present design approach which combines both methodologies of maximizing total pressure recovery and prescribing Mach number at the beginning of isolator gives a better total pressure recovery when compared to the approach of only maximizing total pressure recovery. Even at higher Mach numbers, this trend is observed and the deviations in the present and previous approaches in the literature are significant.

Figure 4 shows the turning angles obtained at various Mach numbers for different external and internal shock combinations. As the number of shocks increase, the shock strength required to turn the flow decreases and this requires small turning angles. This is the reason that as the number of shocks increases, the turning angles decrease and thereby increasing the length of the scramjet intake. There has to be a balance in the number of shocks required and the intake length, so that required flow ratios are obtained for minimal length of the inlet which results in minimal weight of the scramjet inlet.

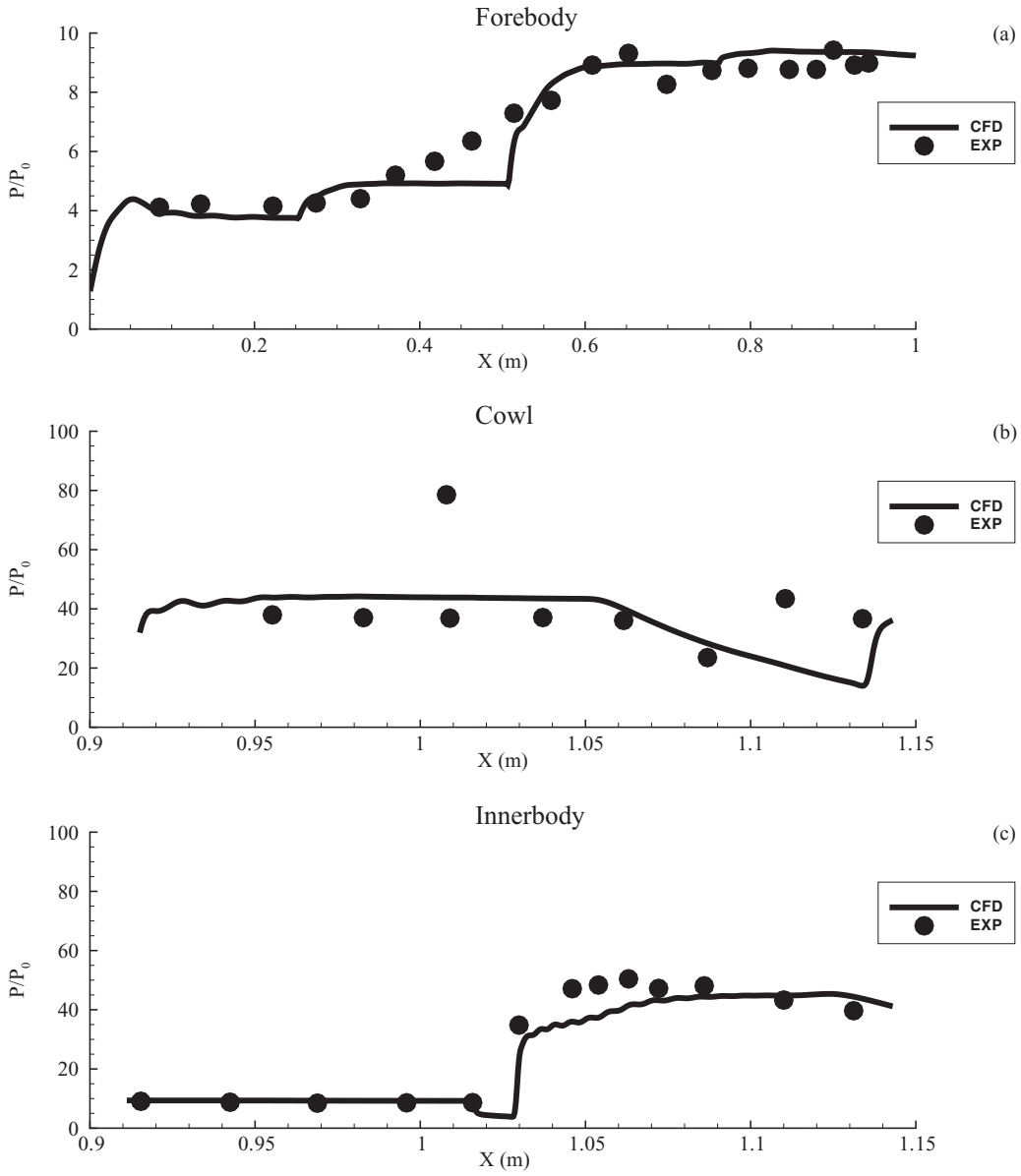

FIG. 5. Pressure distribution along the surface of scramjet inlet.

B. Two-dimensional inviscid and viscous effects

The scramjet inlet flow field involves the study of phenomenon of inviscid/viscous coupling, shock-shock interactions, shock/boundary layer interactions, separation, etc. Computational fluid dynamics is one of the most powerful tools for understanding this phenomena and helps in designing and analyzing the realistic propulsion system. Designed scramjet inlet geometry has been analyzed using CFD and reported here. Accuracy of present numerical methods is tested by validating the experimental results available in the literature.[15] Mach 10 inlet flow field characteristics are obtained with free stream conditions of Mach number $M_1 = 10.4$, static pressure $P_1 = 75647.65$ Pascal, free stream temperature $T_1 = 215$ K and walls with a constant surface temperature $T_w = 1000$ K. Surface static pressure distribution along the forebody, cowl and inner body plotted in Figure 5. Experimental data are shown in discrete symbols and present results are shown in solid lines. Surface static pressure along the forebody is increasing due to external compression shocks. Present results showed an excellent agreement with experimental results of Van Wie and Ault.[15]

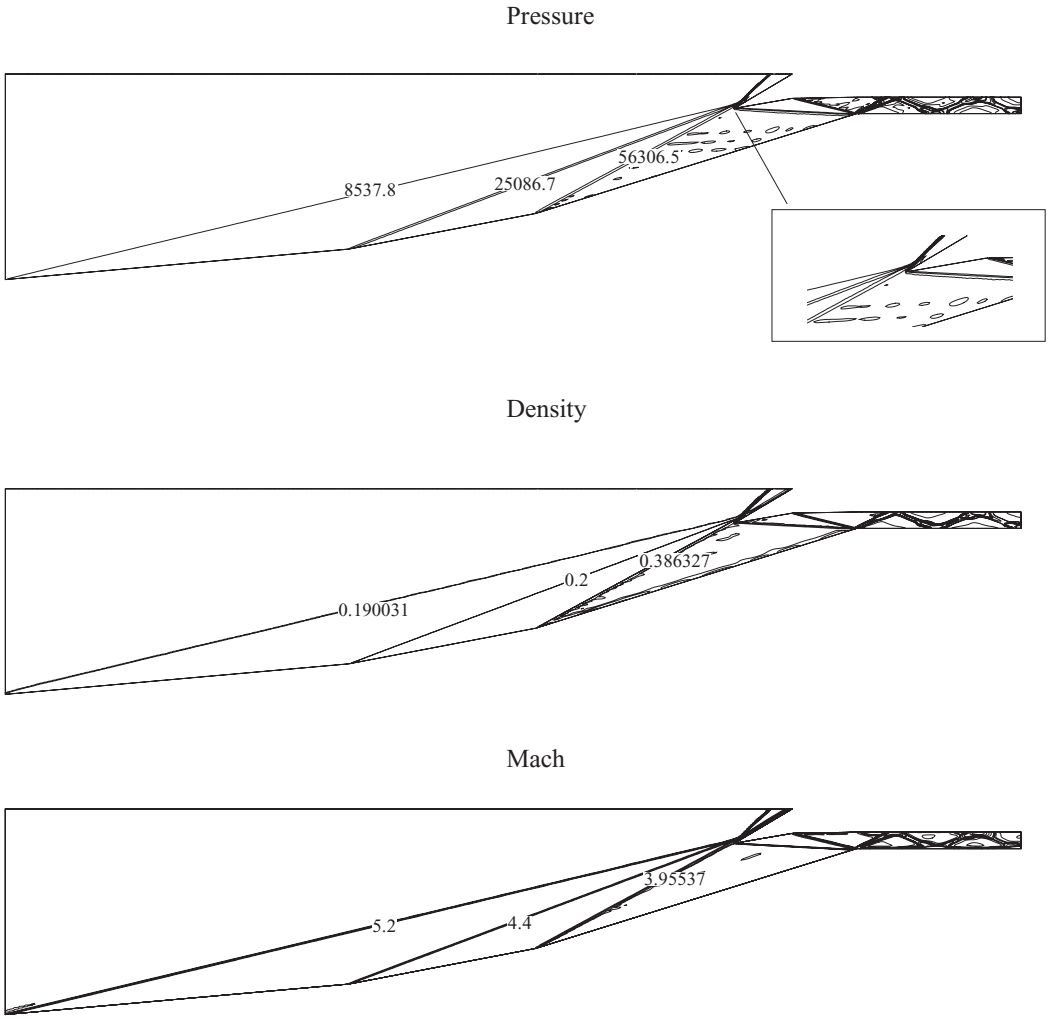

FIG. 6. Pressure, density, and Mach number contours of Mach 6 inlet geometry at Mach 6.

1. 2D inviscid effects

Mach 6 inlet geometry generated by present design procedure is simulated and the flow field characteristics are obtained with free stream conditions of Mach number $M_1 = 6.0$, static pressure $P_1 = 6079.5$ Pascal, free stream temperature $T_1 = 230$ K and walls with a constant surface temperature $T_w = 1000$ K. The isolator length is chosen as ten times the width of the isolator. Pressure, density and Mach number contours are shown in Figure 6 for the above operating conditions. In Figure 6, contours are plotted at quasisteady state condition, i.e., when the solution is not changing with increase in time. From Figure 6, it is seen that *shock-on-lip* condition is not satisfied even though geometry generated by imposing this condition. The design procedure is based on one-dimensional inviscid gas dynamic relations and hence causes deviations in the flow field when two-dimensional effects are considered. The static pressure and density increases along the inlet due to compression process by oblique shocks. The inlet is converting kinetic energy of the incoming fluid into pressure energy which results in decrease of Mach number along the inlet. Internal shocks get deflected from the beginning of the isolator and propagate into the isolator section as series of shock reflections, further increasing the static pressure ratio.

Mach 6 scramjet inlet performance parameters such as SPR, TPR and Mach number at the beginning of isolator are given in Table I for 1D, 2D inviscid and 2D viscous analysis. As per the design procedure TPR at the beginning of isolator is 0.864 for Mach 6 inlet. The TPR at the beginning

TABLE I. Performance parameters of Mach 6 inlet geometry for 1D, 2D inviscid and viscous effects.

Mach	6(1D Inviscid)	6(2D Inviscid)	6(Viscous)	6.5(2D Inviscid)	6.5(Viscous)
SPR_{is}	35.49	39.81	48.23	45.06	50.8
TPR_{is}	0.864	0.825	0.684	0.75	0.675
M_{is}	3	2.94	2.67	3.14	2.94
SPR_{exit}	...	40.272	51.506	44.69	56.046
TPR_{exit}	...	0.8105	0.5107	0.73	0.5277
M_{exit}	...	2.9251	2.45	3.124	2.726

of isolator has decreased from 0.864 to 0.825 when two-dimensional effects are considered which shows that two-dimensional effects have to be considered for the design of scramjet inlet. It can be noticed that TPR has further decreased in the isolator section. Even though TPR has decreased in the isolator, it is needed to avoid the back pressures entering from the combustion chamber to the inlet. If the inlet is operated above design Mach number corresponding shock angles decrease and converge on or below the cowl lip. Internal shocks are pushed into the isolator section, where they continue further downstream with uneven shock reflections leading to flow non-uniformity. This has been observed when Mach 6 inlet is operated at Mach 6.5 and shown in Figure 7. From Figure 7, It is noticed that shocks do not converge on cowl lip which indicates that *shock-on-lip* condition is not satisfied. The total pressure recovery at the beginning of isolator has decreased from 0.825 to 0.75 with increase in free stream Mach number from 6 to 6.5.

By using the same design procedure Mach 8 geometry is designed and then simulated at different free stream Mach numbers. Mach 8 inlet performance parameters are given in Table II and similar characteristics as of Mach 6 are observed.

2. Viscous effects

Mach 6 inlet flow field is simulated for viscous and turbulent effects and is plotted in Figure 8 at design free stream Mach number. From Figure 8, it is noticed that there is a considerable deviation in converging position of shocks in viscous analysis compared to inviscid analysis as shown in Figure 6 due to boundary layer effects and shock wave/boundary layer interactions. From Figure 8, the *shock-on-lip* condition is not satisfied even though inlet geometry is generated by imposing this condition. The TPR at the beginning of isolator has decreased from 0.825 to 0.684 when viscous effects are considered as given in Table I. Mach 6 inlet flow field characteristics are shown in Figure 9 at the free stream Mach number 6.5. From Figure 9, the external shocks are converging on cowl lip which indicates that inlet has satisfied the *shock-on-lip* condition at Mach 6.5 instead of design Mach number 6. If the inlet satisfies the *shock-on-lip* condition it ensures maximum capture area, minimum intake length and improves the compression process. The Mach 6 inlet performance parameters are given in Table I. In the tables, the subscripts "is" and "exit" indicates the beginning and exit of the isolator. From Table I, inlet efficiency is high in inviscid case but these cannot be considered as in the real scenario the scramjet operates in a completely viscous environment.

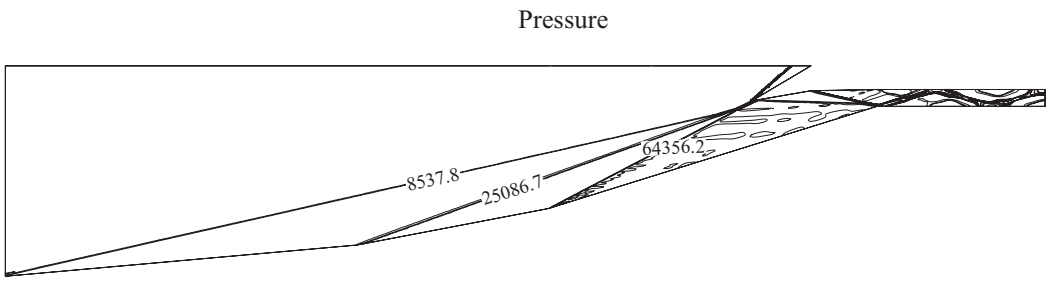

FIG. 7. Pressure contours of Mach 6 inlet geometry at Mach 6.5.

TABLE II. Performance parameters of Mach 8 inlet geometry for 1D, 2D inviscid and viscous effects.

Mach	8(1D Inviscid)	8(2D Inviscid)	8(Viscous)	9(2D Inviscid)	9(Viscous)
SPR_{is}	50.05	66.41	72.99	68.3	75.97
TPR_{is}	0.829	0.68	0.53	0.628	0.56
M_{is}	4	3.75	3.46	4.3	4.02
SPR_{exit}	...	64.94	79.895	65.93	87.746
TPR_{exit}	...	0.620	0.322	0.596	0.385
M_{exit}	...	3.7	3.179	4.261	3.732

Pressure contours of Mach 8 inlet at different free stream Mach number are shown in Figures 10 and 11. From Figure 11, the external shocks are converging on cowl lip at Mach 9 instead of design Mach number 8. The Mach 8 inlet performance parameters are given in Table II. The TPR at the beginning of isolator has decreased from 0.628 to 0.56 when viscous effects are considered for Mach 8 inlet operated at Mach 9. The static pressure increases along the inlet due to compression process by oblique shocks and correspondingly decreases Mach number along the inlet.

C. Correction factor in design for viscous effects

As seen in Sec. IV B 2, when viscous effects are included, the *shock-on-lip* condition is not satisfied at design free stream Mach number. Scramjet inlet has to be operated above the design free stream Mach number in order to satisfy the *shock-on-lip* condition. For example, Mach 6 and Mach 8 inlets have to operate at Mach 6.5 and Mach 9 to satisfy the *shock-on-lip* condition. This means that inviscid design algorithm to be modified to include the viscous effects. This aspect has been investigated at different inlets with different design Mach numbers and found that design Mach number is in linear relation with actual Mach number (M_{actual}), i.e., Mach number at which *shock-on-lip* condition is satisfied as shown in Figure 12. From Figure 12, the linear fit equation has been obtained as $M_{actual} = 1.22M_{design} - 0.799$. This correction can be included in the inviscid algorithm to obtain the actual operating free stream Mach number at which *shock-on-lip* condition is satisfied. In order to test the above relation, two scramjet inlets are designed at $M_{design} = 5$, 10 and simulated at $M_{actual} = 5.311$, 11.421, respectively, as given by the above relation. The pressure contours of these results are shown in Figures 13 and 14. As predicted, the scramjet inlets satisfy the *shock-on-lip* condition at M_{actual} given by the relation rather than at design Mach number M_{design}. So the actual operating free stream Mach number relation will be very useful for design of scramjet inlets.

D. Parametric study of M_e and M_{is}

Mach number after external compression (M_e) and Mach number at the beginning of isolator (M_{is}) are important parameters for design and determines the inlet flow behavior of scramjet inlet. Amount of compression required and compression efficiency is dependent on these parameters. In

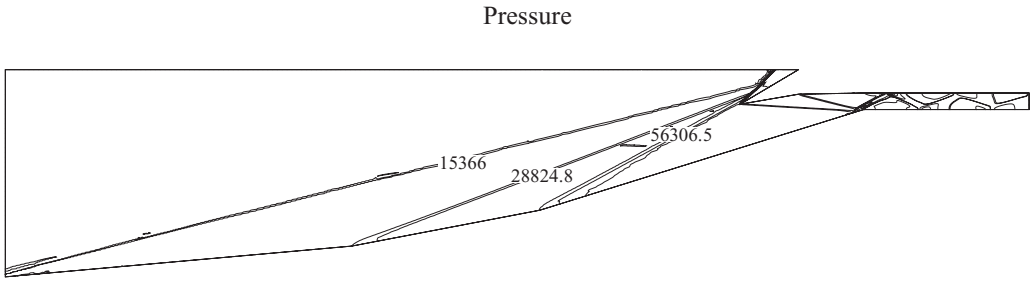

FIG. 8. Pressure contours of Mach 6 inlet geometry at Mach 6 for viscous effects.

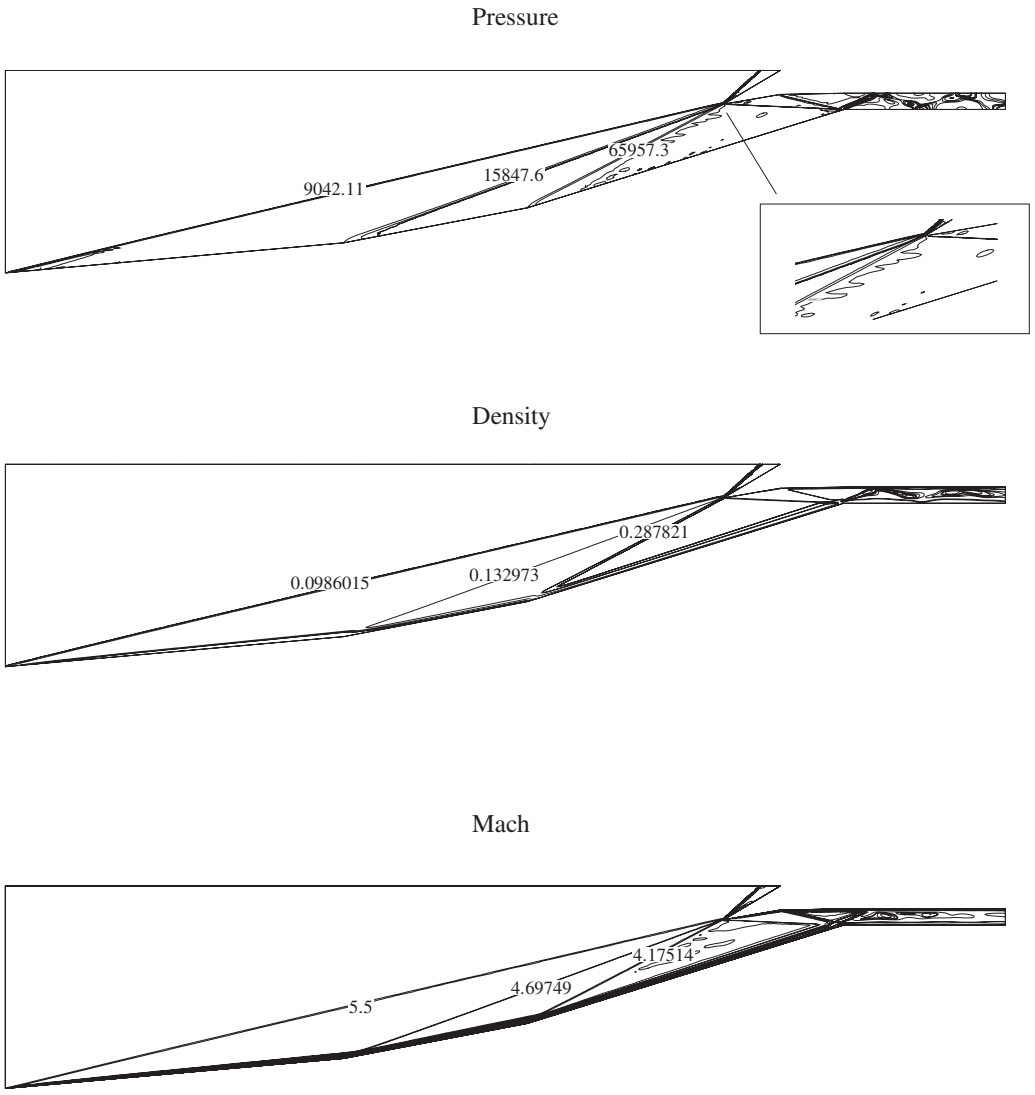

FIG. 9. Pressure, density, and Mach number contours of Mach 6 inlet geometry at Mach 6.5 for viscous effects.

order to know the effects of these parameters on the total pressure recovery, a parametric study is carried out using gas dynamic relations. When M_{is} is fixed and M_e is varied from 99% of M_1 to 1% of M_1, it is found that total pressure is maximum for a certain range of Mach numbers. This range varies from 67% of M_1 to 73% of M_1 for M_{is} = 50% of M_1 and 65% of M_1 to 71% of M_1 for M_{is} = 40% of M_1 at different free stream Mach numbers. These effects are shown in Figure 15. This

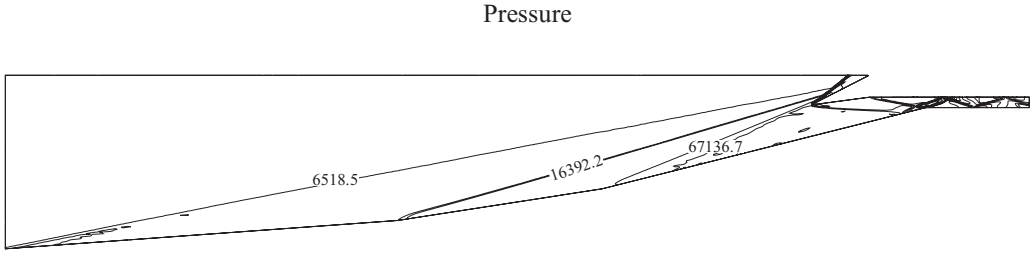

FIG. 10. Pressure contours of Mach 8 inlet geometry at Mach 8 for viscous effects.

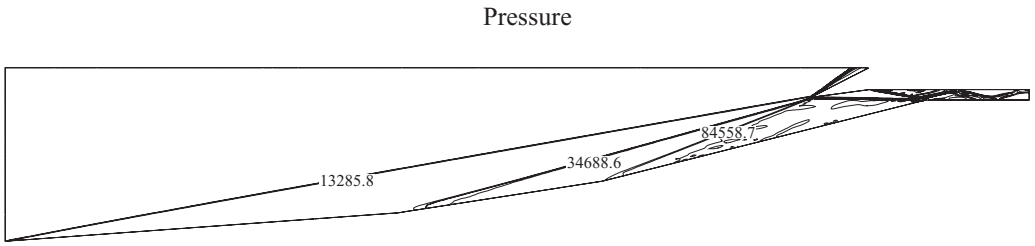

FIG. 11. Pressure contours of Mach 8 inlet geometry at Mach 9 for viscous effects.

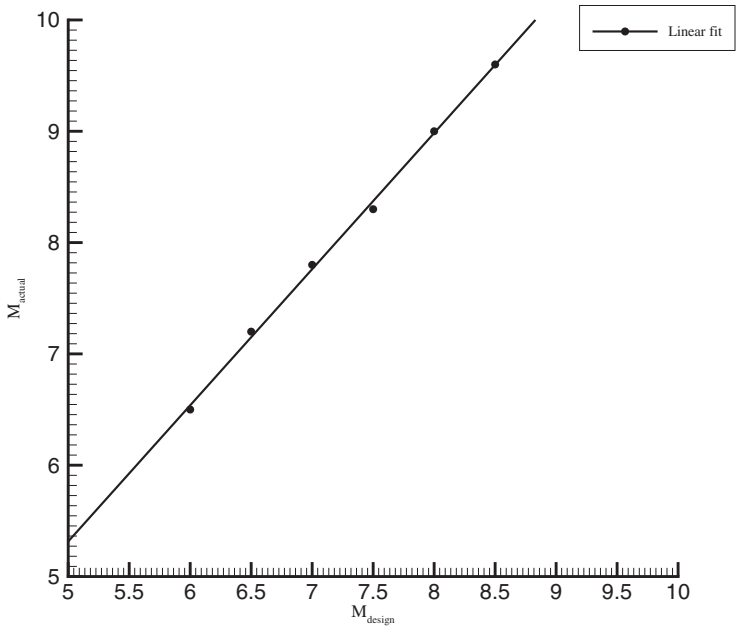

FIG. 12. Deviation of actual Mach number from design Mach number.

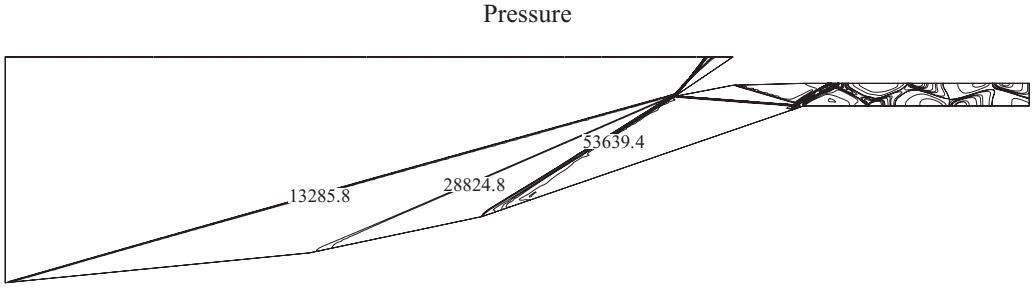

FIG. 13. Pressure contours of Mach 5 inlet geometry operated at Mach 5.311.

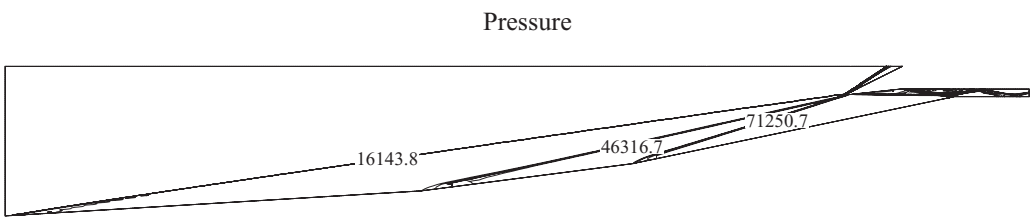

FIG. 14. Pressure contours of Mach 10 inlet geometry operated at Mach 11.421.

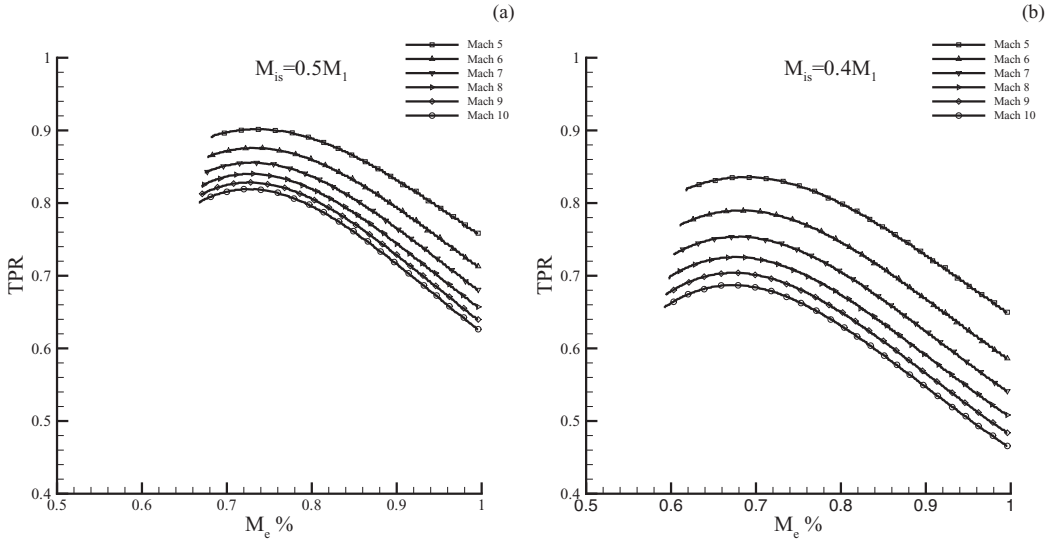

FIG. 15. Variation of TPR with M_e at the beginning of isolator Mach numbers $M_{is} = 50\%\ M_1$ and $M_{is} = 40\%M_1$.

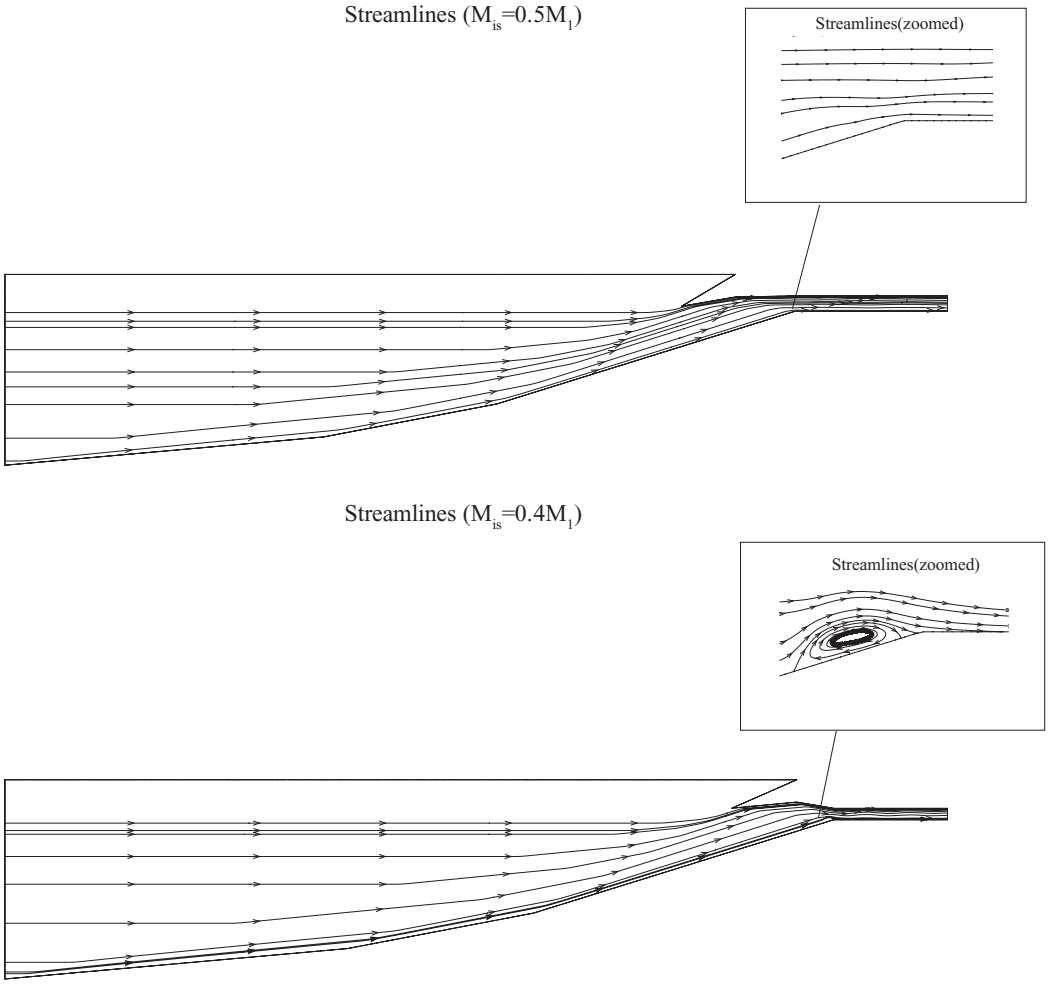

FIG. 16. Streamline contours of Mach 6 inlet geometry operated at Mach 6.5 for different Mach numbers at the beginning of isolator.

might be due to the reason that as M_e increases, external shocks have to turn flow lesser and requires low strength shocks and there by puts additional load on the internal shocks by increasing their shocks strengths. Hence this leads to decrease in total pressure recovery as to the strength of the shock is inversely proportional to the total pressure recovery across the shock. Also, M_e cannot be decreased after certain limit as the flow turns sonic, due to occurrence of normal shock and hence no oblique shock solution exists. So the present design has chosen the optimum value of $M_e = 68\%$ of M_1.

The total pressure recovery decreases with decrease of Mach number at the beginning of isolator M_{is} from 50% to 40 % of M_1. Hence it is desirable to fix the Mach number at the beginning of isolator as 50% of free stream Mach number M_1. Of course higher efficiencies might exist at higher Mach numbers at the beginning of isolator, higher Mach numbers at the beginning of isolator implies to low static pressure ratio which leads to inefficient compression. Therefore, an optimal pressure ratio is a key component in achieving adequate compression. Two scramjet inlets are designed at Mach 6 with a different Mach numbers at the beginning of isolator $M_{is}= 40\%$ of M_1 and $M_{is}= 50\%$ of M_1 and simulated at a free stream Mach number of $M_1 = 6.5$. The stream line contours are plotted in Figure 16. A separation region observed near the beginning of isolator for the case of $M_{is}= 40\%$ of M_1 as reported in the literature.[10] As the Mach number at the beginning of isolator is decreased which means shock strength has to be increased leading to back pressure and flow turns to backwards.

V. CONCLUSIONS

A new methodology has been developed for the design of hypersonic scramjet inlet and reported here. Study of scramjet intakes is vital for future space transportation and hypersonic flight applications. In the literature design of scramjet inlet has been done by either maximize the total pressure recovery or prescribing Mach number at the beginning of isolator. Present investigation has combined the above two approaches and obtained the optimal inlet geometry which has maximum total pressure recovery at a prescribed free stream Mach number. Designed scramjet inlet geometries are simulated and performance parameters are reported for various parameters such as 1D, 2D invsicid and viscous effects. Present simulations are able to capture the flow field characteristics such as oblique shocks, shock/boundary layer interactions, and shock reflections.

Total pressure recovery which determines the inlet efficiency is higher in the present approach than the previous approaches. Turning angles decrease with an increase of external/internal shocks due to decrease of shock strength. The efficiency of the inlet increases with an increase of external/internal shocks. There is a significant deviation in performance parameters of inlet in 1D, 2D inviscid and viscous analysis. Present results show that 2D and viscous effects have to be considered for design of scramjet inlets. The *shock-on-lip* condition which is imposed by the design methodology but this does not satisfy in the viscous flow field due to shock-shock and shock/boundary layer interactions. A correction equation is given which finds the actual Mach number that satisfies the *shock-on-lip* condition. Present results agree with the experimental results in the literature.[15] Present results shown that separation region is formed if Mach number at the beginning of isolator is $0.4M_1$ due to increase of shock strength. As predicted in the literature,[10] it is shown that when the Mach number the beginning of isolator is decreased below $50\%M_1$ separation region is developed. The present approach will be useful for the design of hypersonic inlets.

[1] E. T. Curran and S. N. B. Murthy, *Scramjet Propulsion*, Progress in Astronautics and Aeronautics Vol. 189 (AIAA, 2000).
[2] W. H. Heiser and D. T. Pratt, *Hypersonic Air Breathing Propulsion* (AIAA, 1993).
[3] M. Valorani, F. Nasuti, M. Onofri, and C. Buongiorno, "Optimal supersonic intake design for air collection engines," Acta Astronaut. **45**(12), 729–745 (1999).
[4] K. Oswatitsch, *Pressure Recovery for Missiles with Reaction Propulsion at High Supersonic Speeds (the Efficiency of Shock Diffusers)*, TM 1140 (translation) (NACA, 1947).
[5] M. K. Smart, "Optimization of two dimensional scramjet inlets," J. Aircr. **36**(2), 430–433 (1999).
[6] X. Xu, X. Dajun, and C. Guobio, "Optimization design for scramjet and anlaysis of its operation performance," Acta Astronaut. **57**, 390–403 (2005).
[7] A. Kantrowitz and C. Donaldson, *Preliminary Investigation of Supersonic Diffusers*, WRL-713 (NACA, 1948).
[8] M. K. Smart and C. A. Trexler, "Mach 4 performance of a fixed-geometry hypersonic inlet with rectangular-to-elliptical shape transition," J. Propul. Power **20**(2), 288–293 (2004).
[9] J. M. Delery, "Shock wave/turbulent boundary layer interaction and its control," Prog. Aerosp. Sci. **22**, 209–280 (1985).

[10] J. J. Mahoney, *Inlets for Supersonic Missiles*, AIAA Education Series (AIAA, Washington, DC, 1991).
[11] A. Hamed and J. S. Shang, "Survey of validation database for shockwave boundary layer interactions in supersonic inlets," J. Propul. Power **7**(4), 617–624 (1991).
[12] M. K. Smart, "Design of three-dimensional hypersonic inlets with rectangular-to-elliptical shape transition," J. Propul. Power **15**(3), 408–416 (1999).
[13] M. K. Smart, "Experimental testing of a hypersonic inlet with rectangular-to-elliptical shape transition," J. Propul. Power **17**(2), 276–283 (2001).
[14] J. Haberle and A. Gulhan, "Investigation of two-dimensional scramjet inlet flow field at Mach 7," J. Propul. Power **24**(3), 446–459 (2008).
[15] D. M. Van Wie and D. A. Ault, "Internal flow field characteristics of a scramjet inlet at Mach 10," J. Propul. Power **12**(1), 158–164 (1996).
[16] F. S. Billig and A. P. Kothari, "Stream line tracing: Technique for designing hypersonic vehicles," J. Propul. Power **16**(3), 465–471 (2000).
[17] B. U. Reinartz and C. D. Hermann, "Aerodynamic performance analysis of a hypersonic inlet isolator using computation and experiment," J. Propul. Power **19**(5), 868–875 (2003).
[18] L. A. Povinelli, *Advanced Computational Techniques for Hypersonic Propulsion*, TM-102005 (NASA, 1989).
[19] S. Shu, Z. Hongying, C. Keming, and W. Yizhao, "The full flowpath analysis of a hypersonic vehicle," Chin. J. Aeronaut. **20**, 385–393 (2007) .
[20] M. E. White, J. P. Drummond, and A. Kumar, "Evolution and application of CFD techniques for scramjet engine analysis," J. Propul. Power **3**(5), 423–439 (1987).
[21] C. E. Cockrell, and L. D. Huebner, "Generic hypersonic inlet module analysis," AIAA Paper No. 91-3209, 1991.
[22] D. R. Reddy, G. E. Smith, M. F. Liou, and T. J. Benson, *Three Dimensional Viscous Analysis of a Hypersonic Inlet*, TM-101474 (NASA, 1989).
[23] S. D. Holland, *Mach 10 Computational Study of a Three-Dimensional Scramjet Inlet Flow Field*, TM-4602 (NASA, 1995).
[24] Z. A. Rana, B. Thornber, and D. Drikakis, "Transverse jet injection into a supersonic turbulent cross-flow," Phys. Fluids **23**, 046103 (2011).